JAERI-M
83-148

A DESIGN OF A MODE CONVERTER FOR ELECTRON CYCLOTRON HEATING BY THE METHOD OF NORMAL MODE EXPANSION

September 1983

Katsumichi HOSHINO, Hisato KAWASHIMA,
Kenichiro HATA* and Takumi YAMAMOTO

日本原子力研究所
Japan Atomic Energy Research Institute

編集兼発行　日本原子力研究所
印　　刷　山田軽印刷所

A Design of a Mode Converter for Electron Cyclotron Heating by the Method of Normal Mode Expansion

Katsumichi HOSHINO, Hisato KAWASHIMA, Kenichiro HATA*
and Takumi YAMAMOTO

Department of Thermonuclear Fusion Research,
Tokai Research Establishment, JAERI

(Received August 12, 1983)

Mode conversion of electromagnetic wave propagating in the over-size circular waveguide is attained by giving a periodical perturbation in the guide wall. Mode coupling equation is expressed by "generalized telegraphist's equations" which are derived from the Maxwell's equations using a normal mode expansion.

A computer code to solve the coupling equations is developed and mode amplitude, conversion efficiency, etc. of a particular type of mode converter for the 60 GHz electron cyclotron heating are obtained.

Keywords : Mode Converter, Electron Cyclotron Heating, Equation, Telegraphy, Microwave Circuit, Coupling Equations

* On leave from Nuclear Energy Data Center

JAERI-M 83-148

固有モード展開法による電子サイクロトロン加熱用モード変換器の設計

日本原子力研究所東海研究所核融合研究部
星野　克道・川島　寿人・畑　健一郎*
山本　巧

（1983年8月12日受理）

円形導波管壁に周期的な摂動を加えることにより，オーバーサイズ導波管内の伝播モードを変換することができる。モード結合方程式は，“一般化された電信方程式”で表わされ，それは固有モード展開を用いてマクスウェル方程式から導かれたものである。

この結合方程式を解く計算機コードが開発され，60GHz 電子サイクロトロン加熱用のモード変換器のモード振幅，変換効率その他の特性が得られた。

---

* 業務委託要員；原子力データセンタ

Contents

目　　次

1. Introduction

The recent development of high frequency ($\gtrsim$ 60 GHz), high power ($\gtrsim$ 200 kW) microwave source called 'gyrotron' enables us to apply the electron cyclotron heating (ECH) to the medium size tokamak machine such as JFT-2M.

The power loss during transfer of the microwave from the source to the tokamak machine is a serious problem in such high frequency. The gyrotron generates the wave of circular TE_{02} mode, but from the consideration of the guide loss and conversion loss at the bend, TE_{01} mode is preferable. Therefore, a need of $TE_{02} \rightarrow TE_{01}$ mode converter arises.

There is a need of another mode converter. For the efficient coupling of wave power to plasma electrons at the electron cyclotron resonance layer, it is preferable to launch linear mode or elliptical mode from antenna. These modes correspond to plasma modes which propagate at specified angle to the tokamak magnetic field. $TE_{01} \rightarrow TE_{11}$ mode converter is necessary for the purpose.

Mode converters which have periodical perturbation in the guide wall have been proposed.[1)] These converters have perturbation which has wave number that is the difference of the wave number of the input mode and output mode. The shape of them is shown in Fig. 1.

For $TE_{02} \rightarrow TE_{01}$ mode conversion, perturbation is the radial one, and radial mode number is changed from 2 to 1. For $TE_{01} \rightarrow TE_{11}$ mode conversion, azimuthal perturbation is imposed, and azimuthal mode number is raised from 0 to 1. $TE_{02} \rightarrow TE_{01}$ converter has a dumbbell shape, whereas $TE_{01} \rightarrow TE_{11}$ converter has a meander shape.

For simplicity, sine curve is adoped as a function of the perturbation.

The wave number (k) of the perturbation is expressed as

$$k = \frac{2\pi}{\lambda} = |k_{mn} - k_{m'n'}| \qquad (1)$$

where

λ ; wave length of the perturbation

k_{mn}; wave number of TE_{mn} or TM_{mn} mode

$k_{m'n'}$; wave number of $TE_{m'n'}$ or $TM_{m'n'}$ mode

$$k_{mn} = \sqrt{k_0^2 - \chi_{mn}^2} \tag{2}$$

$$k_0 = \frac{\omega}{c} = \frac{2\pi\nu}{c} \tag{3}$$

$$\chi_{mn} = \begin{cases} \dfrac{p'_{mn}}{a} & \text{for TE mode} \\ \dfrac{p_{mn}}{a} & \text{for TM mode} \end{cases} \tag{4}$$

c ; velocity of light in vacuum

ν ; frequency

a ; radius of the circular wave guide

p'_{mn}; n-th zero of the differential of the Bessel function $J'_m(x)$

p_{mn}; n-th zero of the Bessel function $J_m(x)$.

For example, we take ν = 59.7 GHz. Then λ is obtained using eq. (1) ~ (4) as

① λ = 8.32 cm for $TE_{02} \rightarrow TE_{01}$ conversion at 2a = 2.78 cm (1.094 inch)

② λ = 12.2 cm for $TE_{01} \rightarrow TE_{11}$ conversion at 2a = 1.91 cm (0.750 inch).

Mode coupling equations should be solved to obtain the mode amplitude or mode conversion efficiency which are functions of the perturbation amplitude and length of the converter (or in another words, number of the perturbation).

In the next chapter, the coupling equations are introduced. In Chap 3, description of the computer code is given and results of the computation and discussions are given in Chap. 4.

2. Mode Coupling Equations (Generalized Telegraphist's equations)

The transverse components of the fields in the waveguide are derived from potential functions and stream functions. These functions may be expressed as a series expansion by some ortho-normal eigen functions. We take the natural eigen modes in the circular waveguide as such functions. The boundary condition that tangential component of the electric field at the guide wall vanishes is automatically satisfied by this expansion.

Stream functions π, $\bar{\Psi}$ is expressed as the field pattern. Then transverse field patern T satisfies

$$\nabla^2 T = - \chi^2 T \quad . \tag{5}$$

We expand potential and stream functions by T.

$$V = - \sum_{(m,n)} V_{(mn)} T_{(mn)}$$

$$\pi = - \sum_{(m,n)} I_{(mn)} T_{(mn)}$$

$$\bar{\Psi} = - \sum_{[m,n]} V_{[mn]} T_{[mn]} \tag{6}$$

$$U = - \sum_{[m,n]} I_{[mn]} T_{[mn]}$$

Here (mn) represents the suffix of TM mode and [mn] for TE mode.

The transverse components of the fields are given by

$$E_t = - \text{grad } V - \text{flux } \bar{\Psi} \tag{7}$$

$$H_t = \text{flux } \pi - \text{grad } U \quad .$$

After substituing (7) to the Maxwell's equations and integrating in the guide cross section, one obtains the following coupling equations[2)] in the form of ordinary differential equations called "generalized telegraphist's equations" in which Z represents the coordinate, $A_{(mn)}$, $A_{[mn]}$ represents foward wave amplitude of TM wave or TE wave and $B_{[mn]}$, $B_{(mn)}$ represents backward wave amplitude respectively.

$$\frac{dA_{[mn]}}{dZ} = -i \sum_{m'n'} \left[k^{+[m'n']}_{[mn]} A_{[m'n']} + k^{-[m'n']}_{[mn]} B_{[m'n']} \right.$$

$$\left. + k^{+(m'n')}_{[mn]} A_{(m'n')} + k^{-(m'n')}_{[mn]} B_{(m'n')} \right]$$

$$\frac{dB_{[mn]}}{dZ} = +i \sum_{m'n'} \left[k^{-[m'n']}_{[mn]} A_{[m'n']} + k^{+[m'n']}_{[mn]} B_{[m'n']} \right.$$

$$\left. + k^{-(m'n')}_{[mn]} A_{(m'n')} + k^{+(m'n')}_{[mn]} B_{(m'n')} \right] \qquad (8)$$

$$\frac{dA_{(mn)}}{dZ} = -i \sum_{m'n'} \left[k^{+[m'n']}_{(mn)} A_{[m'n']} + k^{-[m'n']}_{(mn)} B_{[m'n']} \right.$$

$$\left. + k^{+(m'n')}_{(mn)} A_{(m'n')} + k^{-(m'n')}_{(mn)} B_{(m'n')} \right]$$

$$\frac{dB_{(mn)}}{dZ} = +i \sum_{m'n'} \left[k^{-[m'n']}_{(mn)} A_{[m'n']} + k^{+[m'n']}_{(mn)} B_{[m'n']} \right.$$

$$\left. k^{-(m'n')}_{(mn)} A_{(m'n')} + k^{+(m'n')}_{(mn)} B_{(m'n')} \right]$$

Where k^+, k^- represent coupling coefficients. The self coupling coefficients which have equal subscripts are phase constants:

$$k^{+[mn]}_{[mn]} = h_{[mn]} + \frac{\beta^2 \Delta^{[mn]}_{[mn]}}{2 h_{[mn]}}$$

$$k^{+(mn)}_{(mn)} = h_{(mn)} + \frac{\chi^2_{(mn)} \delta^{(mn)}_{(mn)} + h^2_{(mn)} \Delta^{(mn)}_{(mn)}}{2 h_{(mn)}} \quad . \qquad (9)$$

The coupling coefficients between any two different modes are expressed as follows:

$$k^{\pm[m'n']}_{[mn]} = \frac{1}{2}\left[\frac{\beta^2\,\Xi^{[m'n']}_{[mn]} - \chi_{[mn]}\,\chi_{[m'n']}\,\xi^{[m'n']}_{[mn]}}{\sqrt{h_{[mn]}\,h_{[m'n']}}} \pm \Xi^{[m'n']}_{[mn]}\sqrt{h_{[mn]}\,h_{[m'n']}}\right]$$

$$k^{\pm(m'n')}_{[mn]} = \frac{1}{2}\,\beta\,\Xi^{(m'n')}_{[mn]}\left[\sqrt{\frac{h_{(m'n')}}{h_{[mn]}}} \pm \sqrt{\frac{h_{[mn]}}{h_{(m'n')}}}\right]$$

$$k^{\pm[m'n']}_{(mn)} = \frac{1}{2}\,\beta\,\Xi^{[m'n']}_{(mn)}\left[\sqrt{\frac{h_{(mn)}}{h_{[m'n']}}} \pm \sqrt{\frac{h_{[m'n']}}{h_{(mn)}}}\right] \tag{10}$$

$$k^{\pm(m'n')}_{(mn)} = \frac{1}{2}\left[\sqrt{h_{(mn)}\,h_{(m'n')}}\;\Xi^{(m'n')}_{(mn)} \pm \frac{\beta^2\,\Xi^{(m'n')}_{(mn)} - \chi_{(mn)}\,\chi_{(m'n')}\,\xi^{(m'n')}_{(mn)}}{\sqrt{h_{(mn)}\,h_{(m'n')}}}\right].$$

In eq. (9), (10), following notations are used:

$$h_{(mn)} = \sqrt{\beta^2 - \chi^2_{(mn)}} \quad ; \text{ axial wave number of TM mode}$$

$$h_{[mn]} = \sqrt{\beta^2 - \chi^2_{[mn]}} \quad ; \text{ axial wave number of TE mode} \tag{11}$$

$\beta^2 = \omega^2\,\mu_0\,\varepsilon_0$; total wave number

$\mu_0 = 4\pi \times 10^{-7}$ (H/m)

$\varepsilon_0 = 8.854 \times 10^{-12}$ (F/m)

$$\chi_{(mn)} = \frac{p_{mn}}{a} \quad ; \text{ transverse wave number of TM mode}$$

$$\chi_{[mn]} = \frac{p'_{mn}}{a} \quad ; \text{ transverse wave number of TE mode} \tag{12}$$

We use the general orthogonal curvilinear coordinates (ρ, φ, z) in which ρ represents radius, φ azimuthal angle and z axial coordinate. Ξ , ξ, Δ, δ are functions expressed as integrals in the cross section.

$$\Xi_{[mn]}^{[m'n']} = \int_s \xi \,(\mathrm{grad}\ T_{[mn]})(\mathrm{grad}\ T_{[m'n']})ds \quad \text{etc.}$$

$$\xi_{[mn]}^{[m'n']} = \chi_{[mn]}\ \chi_{[m'n']} \int_s \xi\ T_{[mn]}\ T_{[m'n']}\ ds \quad \text{etc.} \tag{13}$$

$$\Delta_{[mn]}^{[m'n']} = \int_s \delta \,(\mathrm{grad}\ T_{[mn]})(\mathrm{grad}\ T_{[m'n']})ds \quad \text{etc.}$$

$$\delta_{(mn)}^{(m'n')} = \chi_{(mn)}\ \chi_{(m'n')} \int_s \delta\ T_{(mn)}\ T_{(m'n')}\ ds$$

where ξ is a parameter expressed using the radius of curvature of the guide axis (b) and shape function y(z) as

$$\xi = \frac{\rho}{b}\ \cos\varphi$$

$$b = \frac{(1 + y'^2)^{3/2}}{y''} \quad .$$

δ is given by

$$\varepsilon = \varepsilon_0(1 + \delta)$$

Field pattern has the following form;

$$T_{(mn)} = \sqrt{\frac{\varepsilon_n}{\pi}}\ \frac{J_m(\chi_{(mn)}\rho)\ \sin m\varphi}{p_{mn}\ J_{m-1}(p_{mn})}$$

$$T_{[mn]} = \sqrt{\frac{\varepsilon_n}{\pi}}\ \frac{J_m(\chi_{[mn]}\rho)\ \cos m\varphi}{\sqrt{p'^2_{mn} - m^2}\ J_m(p'_{mn})} \tag{14}$$

where

$$\varepsilon_n = \begin{cases} 1 & m = 0 \\ 2 & m \neq 0 \end{cases} \quad .$$

3. Computer Code MODECONV

A computer code (name ; MODECONV) to solve the coupling equations (8) is described in this chapter.

3.1 Simplified Equations

A general form of the coupling equations is given in chap 2. Simplified equations neglecting the dielectric loss are used in the code.

For the calculation of $TE_{02} \rightarrow TE_{01}$ mode converter (Fig. 1(a)), mode couplings between TE_{01} to TE_{05} mode are included. Higher modes ($n \geqq 6$) are cutoff in our case. The simplified equations are expressed as

$$\begin{aligned}
\frac{dA_{[0n]}}{dZ} &= -i\, h_{[0n]}\, A_{[0n]} - \frac{1}{2}\frac{Kn'}{Kn} B_{[0n]} + \sum_{n'}\left[k^{+[0n']}_{[0n]} A_{[0n']} + k^{-[0n']}_{[0n]} B_{[0n']} \right] \\
\frac{dB_{[0n]}}{dZ} &= i\, h_{[0n]}\, B_{[0n]} - \frac{1}{2}\frac{Kn'}{Kn} A_{[0n]} + \sum_{n'}\left[k^{+[0n']}_{[0n]} B_{[0n']} - k^{-[0n']}_{[0n]} A_{[0n']} \right]
\end{aligned} \tag{15}$$

where the coupling coefficient $k^{\pm}$ are expressed as[3)]

$$k^{\pm[0n']}_{[0n]} = \frac{p'_{0n} \cdot p'_{0n'}}{p'^{\,2}_{0n'} - p'^{\,2}_{0n}} \left[\sqrt{\frac{K_{[0n]}}{K_{[0n']}}} \pm \sqrt{\frac{K_{[0n']}}{K_{[0n]}}} \right] \frac{1}{a}\frac{da}{dZ}$$

$$K_{[0n]} = \frac{\omega\,\mu}{h_{[0n]}} \tag{16}$$

$$K'_{[0n]} = \frac{dK_{[0n]}}{dZ} \quad .$$

---

* Simbols are the same as in Chap 1,2.

For the $TE_{01} \rightarrow TE_{11}$ mode converter (Fig. 1 (b)), mode couplings between TE_{01} and TE_{1n}, TM_{1n} ($n \leq 5$) mode are included. The coupling equations are:

$$\frac{dA_{[01]}}{dZ} = -i\, h_{[01]}\, A_{[01]} - i\, k^{+(11)}_{[01]}\, A_{(11)} - i \sum_{n'} \left[k^{+[1n']}_{[01]}\, A_{[1n']} + k^{-[1n']}_{[01]}\, B_{[1n']} \right]$$

$$\frac{dB_{[01]}}{dZ} = +i\, h_{[01]}\, B_{[01]} + i\, h^{+(11)}_{[01]}\, B_{(11)} + i \sum_{n'} \left[k^{+[1n']}_{[01]}\, B_{[1n']} + k^{-[1n']}_{[01]}\, A_{[1n']} \right]$$

$$\frac{dA_{[1n]}}{dZ} = -i\, h_{[1n]}\, A_{[1n]} - i\, k^{+[01]}_{[1n]}\, A_{[01]} - i\, k^{-[01]}_{[1n]}\, B_{[01]} \tag{17}$$

$$\frac{dB_{[1n]}}{dZ} = +i\, h_{[1n]}\, B_{[1n]} + i\, k^{-[01]}_{[1n]}\, A_{[01]} + i\, k^{+[01]}_{[1n]}\, B_{[01]}$$

$$\frac{dA_{(11)}}{dZ} = -i\, h_{(11)}\, A_{(11)} - i\, k^{+[01]}_{(11)}\, A_{[01]}$$

$$\frac{dB_{(11)}}{dZ} = +i\, h_{(11)}\, B_{(11)} + i\, k^{+[01]}_{(11)}\, B_{[01]} \quad .$$

The coupling coefficients are expressed as

$$k^{\pm(11)}_{[01]} = \frac{1}{2}\, \beta\, \Xi^{(11)}_{[01]} \left[\sqrt{\frac{h_{(11)}}{h_{[01]}}} \pm \sqrt{\frac{h_{[01]}}{h_{(11)}}} \right]$$

$$h_{[01]} = h_{(11)}$$

$$\Xi^{[1n]}_{[01]} = \begin{cases} \dfrac{a}{\sqrt{2}\, p'_{01}\, b} & \text{for} \quad n = 1 \\ 0 & \text{for} \quad n \neq 1 \end{cases}$$

$$k^{+(11)}_{[01]} = \frac{\beta\, a}{\sqrt{2}\, p'_{01}\, b} \tag{18}$$

$$k^{-(11)}_{[01]} = 0$$

$$k^{\pm[1n']}_{[01]} = \frac{1}{2}\left[\frac{\beta^2\, \Xi^{[1n']}_{[01]} - \chi_{[01]}\,\chi_{[1n']}\,\xi^{[1n']}_{[01]}}{\sqrt{h_{[1n']}\, h_{[01]}}} \pm \Xi^{[1n']}_{[01]}\sqrt{h_{[01]}\, h_{[1n']}}\right]$$

$$\xi^{[1n']}_{[01]} = \frac{\sqrt{2}\, a}{b}\;\frac{p'_{1n'}}{\sqrt{p'_{1n'} - 1}}\;\frac{p'^{2}_{01} + p'^{2}_{1n'}}{(p'^{2}_{01} - p'^{2}_{1n'})^2}$$

$$\Xi^{[1n']}_{[01]} = \frac{\sqrt{8}\, a}{b}\;\frac{p'_{01}\quad p'^{2}_{1n'}}{\sqrt{p'^{2}_{1n'} - 1}\,(p'^{2}_{01} - p'^{2}_{1n'})^2} \quad .$$

3.2 Numerical Methods

The ordinary differential equations (eq.(15) or (17)) have the from of

$$y'_n = f\,(x,\, y_n) \quad . \tag{19}$$

We solve (19) with the initial condition

$$y = y_0 \quad \text{when} \quad x = x_0$$

by the Milne's method. Namely, y_n at $x_n = x_0 + nh$ is obtained using the previous four points. Here h is the infinitesimal increment of x. The predictor y^P_n are obtained as

$$y^P_n = y_{n-4} + \frac{4h}{3}\,(2\, f_{n-3} - f_{n-2} + 2\, f_{n-1}) \tag{20}$$

Then using $f_n = f(x,\, y^P_n)$, corrector

$$y_n^c = y_{n-2} + \frac{h}{3} (f_{n-2} + 4 f_{n-1} + f_n) \qquad (21)$$

are obtained. In the next step, new f_n is set as $f_n = (x_n, y_n^c)$, and the new collector is obtained. This successive process is repeated until the collection becomes less than given ε.

In the actual computation, the repeat time is two. If the convergence is not obtained in two times, h is set 1/2 value of the previous value. In the case that correction is less than $\varepsilon/32$, h is set 2 times larger in the next process. The new value of the point in that case is given by Runge-Kutta method.

In the Milne's method, three y's are needed other than the initial value y_0. These are obtained by iteration method as follows.

First, the zero order approximations are obtained from the following formula.

$$\begin{aligned} y_1 &= y_0 + hf(x_0, y_0) \\ y_2 &= y_0 + 2hf(x_1, y_1) \\ y_3 &= y_1 + 2hf(x_2, y_2) \\ y_4 &= y_2 + 2hf(x_3, y_3) \end{aligned} \qquad (22)$$

Then the equations

$$\begin{aligned} y_1 &= y_0 + h(251f_0 + 646f_1 - 264f_2 + 106f_3 - 19f_4)/720 \\ y_2 &= y_0 + h(29f_0 + 124f_1 + 24f_2 + 4f_3 - f_4)/90 \\ y_3 &= y_0 + h(27f_0 + 102f_1 + 72f_2 + 42f_3 - 3f_4)/80 \\ y_4 &= y_0 + h(14f_0 + 64f_1 + 24f_2 + 64f_3 + 14f_4)/45 \end{aligned} \qquad (23)$$

are used repeatedly until the convergence is obtained.

3.3 Construction of the Code

Flow diagram of the code is shown in Fig. 2. Data check is performed to confirm that inappropriate modes or cutoff modes are not set in the data. The result of the calculation is made in a graph by the laser printer.

Parameters of input and output are given in Table 1 and Table 2. In the output are given data input, energy of a certain modes as the square of the wave amplitude. Differential coefficients, width of step h are also given in the output.

In Fig. 3, a tree of the subroutines is given. Functions of each subroutines are as follows:

MAIN	;	read title, and control the calculation
AINTSS	;	read input data for calculation
MODEIN	;	input of the kind of modes
PAREIN	;	grouping of the data
REAMI2	;	input of integer by free format
MDCHK	;	check of the mode input
NUCHK	;	check of the cutoff mode
BCINIT	;	calculation of $\chi_{[mn]}$, $\chi_{(mn)}$, β, $h_{[mn]}$, $h_{(mn)}$
MILNE	;	solve the ordinary differential equation by Milne's method
MINITE	;	obtain 3 points from the initial value for the Milne's method
XSUB	;	calculate differential coefficients
ASUB	;	calculate coupling coefficients of $TE_{02} \rightarrow TE_{01}$ mode converter
BSUB	;	calculate coupling coefficients of $TE_{01} \rightarrow TE_{11}$ mode converter
XOUT	;	output of the result
RK	;	Ruge-Kutta method
GRAPH	;	read graph control data and make graphs
GRMODE	;	select the modes to be expressed in the graph
AZFUNC	;	calculate the shape of the mode converter
LIB	;	library routine codes (PLOTS, PLOT, NEWPEN, SYMBOL, NUMBER) used for graph output

4. Results of the Computation and Discussions

4.1 Outline

The results of the design of mode converter using the MODECONV code are given in this chapter.

With the given frequency (ν) and given radius of the circular wave guide (a), wave length of the perturbation (λ) necessary is decided by eq.(1). Then remaining parameter is amplitude of the perturbation (δ). In determining size of the converters, we take δ as parameter and find required δ and length (Z) of the converter.

We find, λ-dependence and ν-dependence of conversion effeciency (f), and find the accuracy imposed to fabricate the converters.

4.2 Determination of Size of the Converters

In Fig. 4, Z dependence of the conversion efficiency (f) and shape of the mode converter are given. As shown, f is a periodical function of Z. The reflected power was very small (a few orders smaller than foward power).

In Fig. 5, both f as a function of δ and Z_{max} which gives the maximum f are shown.

As δ becomes large, f decreases and amplitude to the parasitic modes increases, but the length (Z) needed to obtain a certain f decreases.

From these considerations, the optimum parameters of the size of the mode converters appricable to the JFT-2M are obtained in Table 3. Here, the length of $TE_{01} \rightarrow TE_{11}$ converter is about the maximum which can installable in the JFT-2M vacuum chamber.

4.3 Frequency-characteristics

Full half width of f is 10.0 GH_Z in both converters as shown in Fig. 6. Notice that Z_{max} takes a discrete value.

4.4 λ-dependence

Full half width of the coversion efficiency (f) is 18 mm for $TE_{02} \rightarrow TE_{01}$ converter and 21 mm for $TE_{01} \rightarrow TE_{11}$ converter as shown in Fig. 7.

4.5 Accuracy imposed for manufacture

In allowing ±5% or ±1% error, the error allowable to δ and λ are obtained as in Table 4, assuming the geometry of Table 3. As known from the table, in the ±5% error in f, accuracy of 0.2 ~ 0.3 mm in shape of the converters is necessary.

As the $TE_{02} \rightarrow TE_{01}$ converter has an axial symmetry, it may not be difficult to get the accuracy, but as $TE_{01} \rightarrow TE_{11}$ converter has not axial symmetry, it needs some notice to fabricate it.

4.6 Applicability of the Code

In the analysis, it is assumed that guide radius (a) is much less than the radius of the curvature at the guide axis (b), namely,

$$\frac{a}{b} \ll 1.$$

$$b = \frac{(1 + y'^2)^{3/2}}{y''} . \qquad (24)$$

We take the shape of the converter as

$$y = a_o \left(1 + \delta \sin \frac{2\pi Z}{\lambda}\right).$$

Then

$$y' = \frac{2\pi a_o \delta}{\lambda} \cos \frac{2\pi Z}{\lambda} \qquad (25)$$

$$y'' = -\left(\frac{2\pi}{\lambda}\right)^2 a_o \delta \sin \frac{2\pi Z}{\lambda}$$

Minimum of b is obtained at

$$y' = 0 \text{ and } y'' = -\left(\frac{2\pi}{\lambda}\right)^2 a_o \delta \text{ as}$$

$$b_{min} = \frac{1}{\left(\frac{2\pi}{\lambda}\right)^2 a_o \delta} . \qquad (26)$$

Using (26), the condition (24) is rewritten as

$$a_o \delta \ll \frac{\lambda^2}{(2\pi)^2 a} \quad . \tag{27}$$

This means

$$\delta \ll 254 \quad (\%) \tag{28}$$

for $\lambda \approx 10$ cm, $a \approx 1$ cm. In our analysis $\delta \leqq 25\%$ and condition (28) is satisfied.

This code can be used for the design of taper of nonlinear shape or for bends with large bend radius.

At last, we may mention that the effect of dielectrics such as water or oil in the wave guide wall is omitted in our analysis. It may rather be complicated to include the dielectric loss in the analysis.

Conclusions

1. A computer code to design a particular type of mode converter for ECH is developed. The method of normal mode expansion is taken as the principle.

2. Using the code, $TE_{02} \rightarrow TE_{01}$ and $TE_{01} \rightarrow TE_{11}$ mode converters are designed for 60 GH_Z ECH in JFT-2M. We get the conversion efficiency of more than 90% as shown in Table 3. Some characteristics of the converters are predicted and accuracy needed for fabrication is obtained.

Acknowledgements

The motivation of this study was given to one of the authors (K. Hoshino) by, Drs. C.P. Moeller, R. Prater and Prof. S.R. Seshadri during his visit to General Atomic Company. They wishes to thank them very much. Also we wish to acknowledge Drs Y. TANAKA, M. Tanaka, Y. Obata, M. Yoshikawa, A. Tomabechi and Y. Iso for their continuous encouragements.

References

1) Moeller, C.P., GA-A 16784 (1982)
2) Morgan S.P., B.S.T.J. 1209 (1957)
3) Unger, H.G., B.S.T.J. 899 (1958)

Conclusions

1. A computer code to design a particular type of mode converter for ECH is developed. The method of normal mode expansion is taken as the principle.

2. Using the code, $TE_{02} \rightarrow TE_{01}$ and $TE_{01} \rightarrow TE_{11}$ mode converters are designed for 60 GH_Z ECH in JFT-2M. We get the conversion efficiency of more than 90% as shown in Table 3. Some characteristics of the converters are predicted and accuracy needed for fabrication is obtained.

Acknowledgements

The motivation of this study was given to one of the authors (K. Hoshino) by, Drs. C.P. Moeller, R. Prater and Prof. S.R. Seshadri during his visit to General Atomic Company. They wishes to thank them very much. Also we wish to acknowledge Drs Y. TANAKA, M. Tanaka, Y. Obata, M. Yoshikawa, A. Tomabechi and Y. Iso for their continuous encouragements.

References

1) Moeller, C.P., GA-A 16784 (1982)
2) Morgan S.P., B.S.T.J. 1209 (1957)
3) Unger, H.G., B.S.T.J. 899 (1958)

Conclusions

1. A computer code to design a particular type of mode converter for ECH is developed. The method of normal mode expansion is taken as the principle.

2. Using the code, $TE_{02} \rightarrow TE_{01}$ and $TE_{01} \rightarrow TE_{11}$ mode converters are designed for 60 GH_Z ECH in JFT-2M. We get the conversion efficiency of more than 90% as shown in Table 3. Some characteristics of the converters are predicted and accuracy needed for fabrication is obtained.

Acknowledgements

The motivation of this study was given to one of the authors (K. Hoshino) by, Drs. C.P. Moeller, R. Prater and Prof. S.R. Seshadri during his visit to General Atomic Company. They wishes to thank them very much. Also we wish to acknowledge Drs Y. TANAKA, M. Tanaka, Y. Obata, M. Yoshikawa, A. Tomabechi and Y. Iso for their continuous encouragements.

References

1) Moeller, C.P., GA-A 16784 (1982)
2) Morgan S.P., B.S.T.J. 1209 (1957)
3) Unger, H.G., B.S.T.J. 899 (1958)

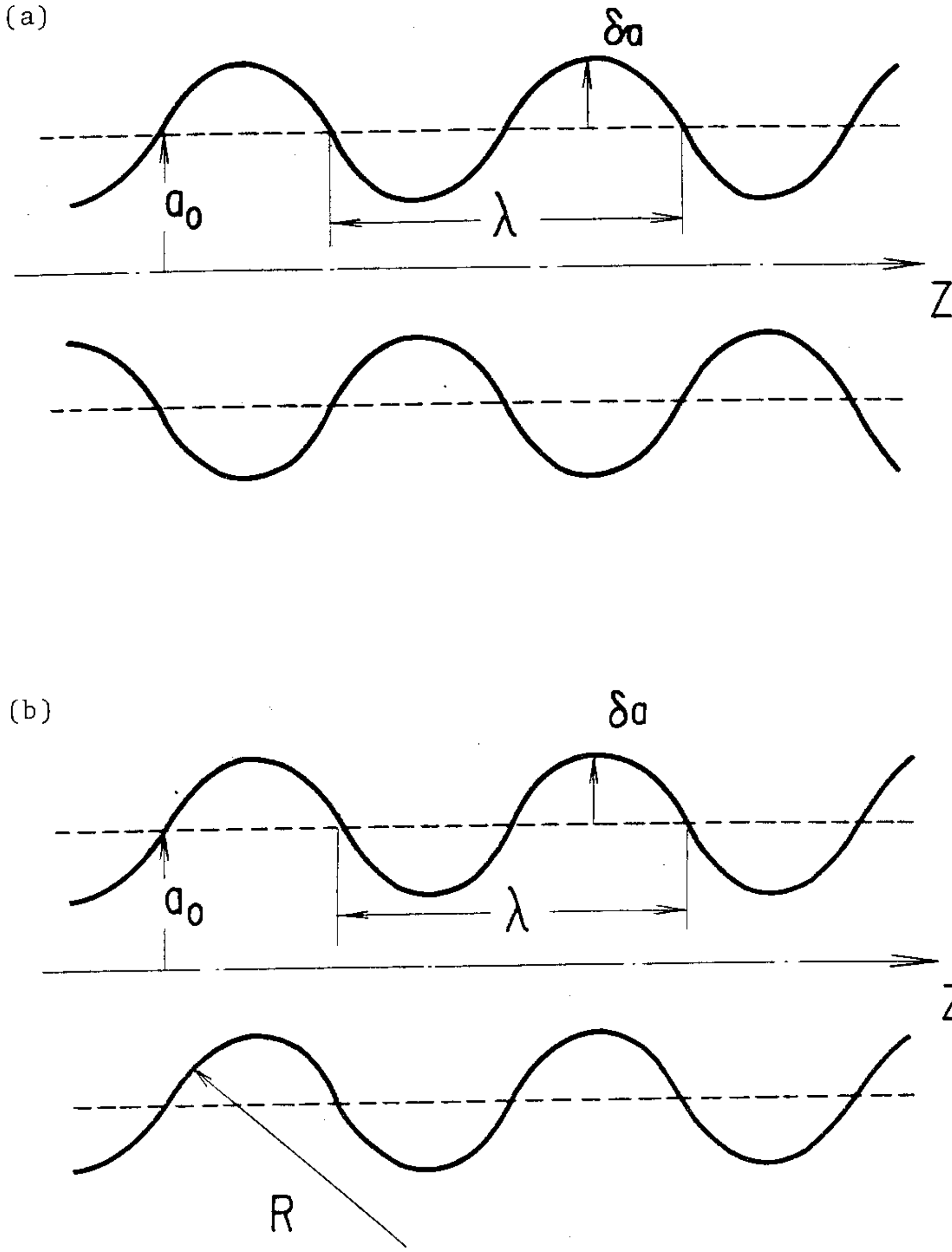

Fig. 1 Shape of the mode converter
(a) $TE_{02} \rightarrow TE_{01}$ converter
(b) $TE_{01} \rightarrow TE_{11}$ converter

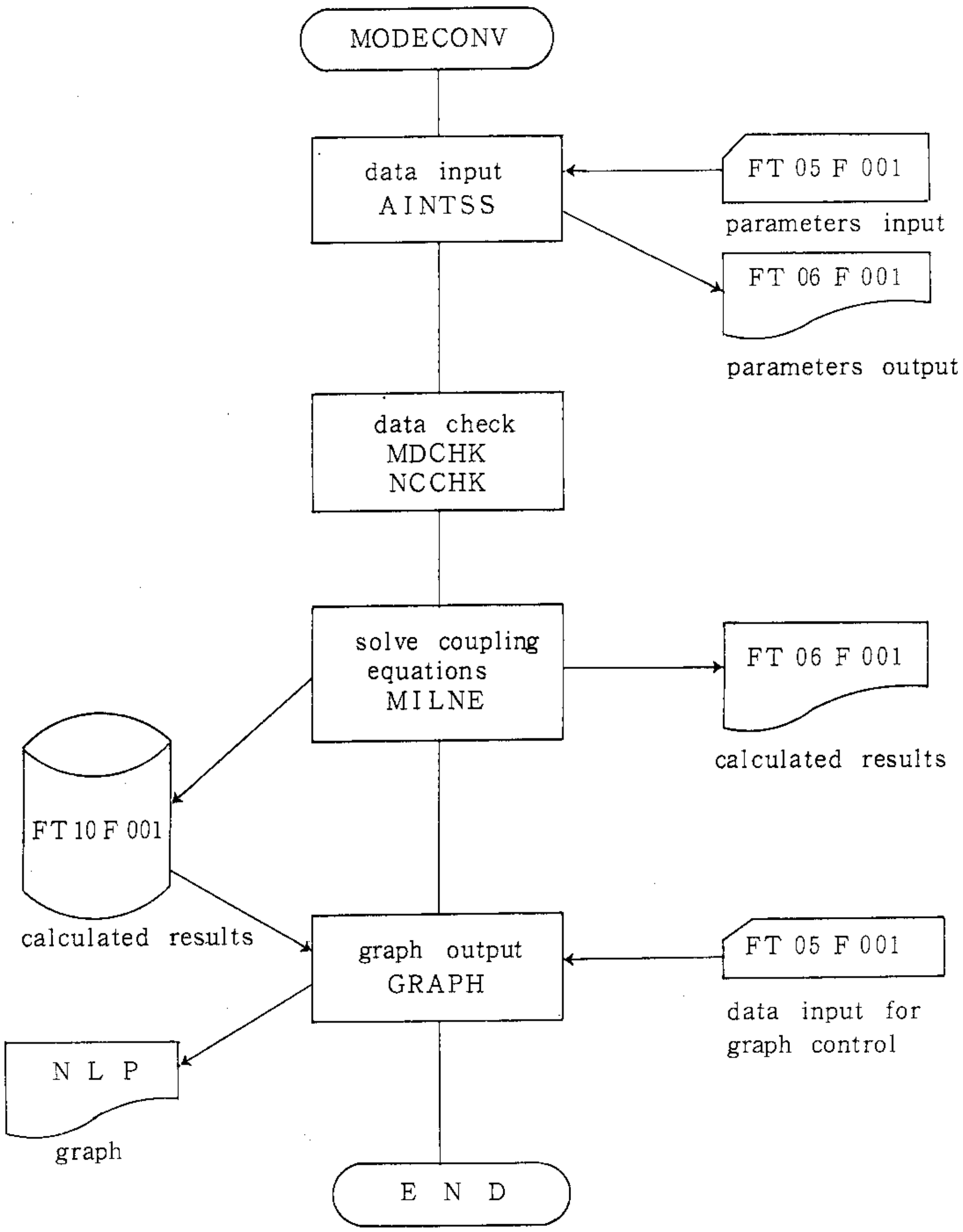

Fig. 2 Data flow diagram of the code

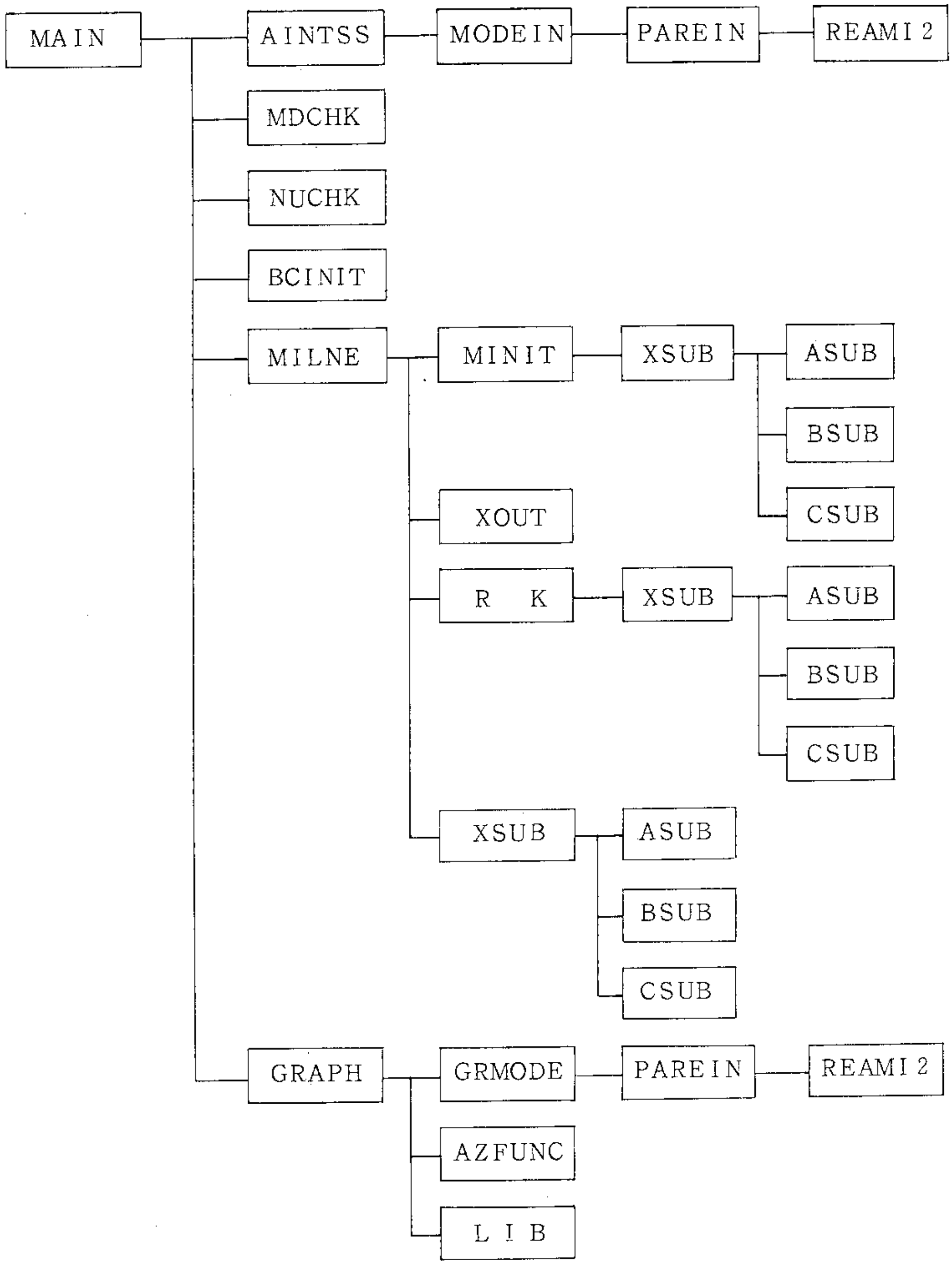

Fig. 3 Tree of the code

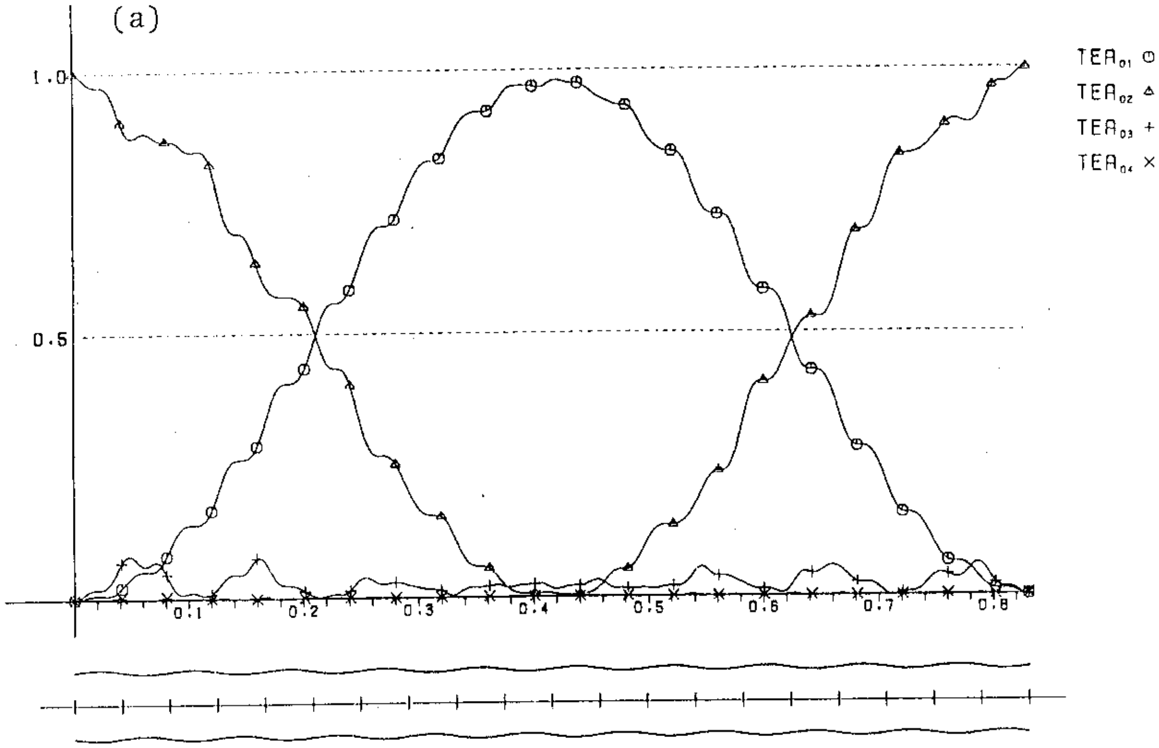

AO = 0.0139 DAO = 6.40% LAMDA = 0.0831

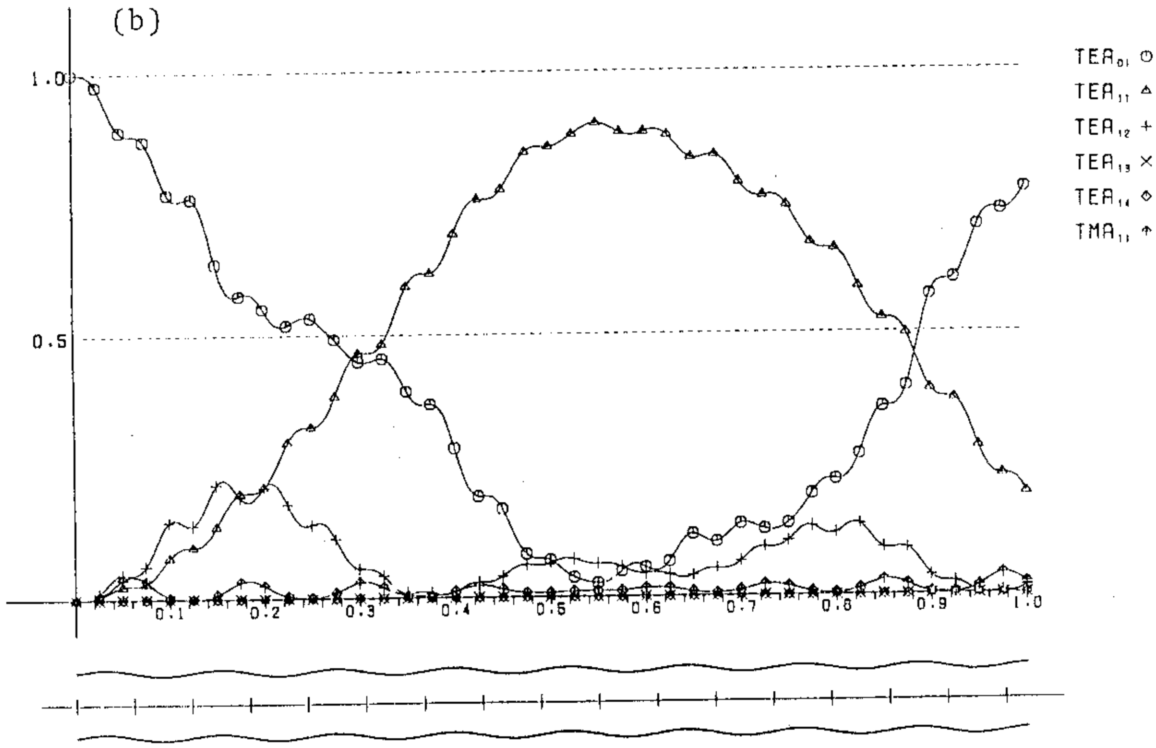

AO = 0.0095 DAO =10.00% LAMDA = 0.1222

Fig. 4 Wave power as the function of Z

(a) $TE_{02} \rightarrow TE_{01}$ converter

(b) $TE_{01} \rightarrow TE_{11}$ converter

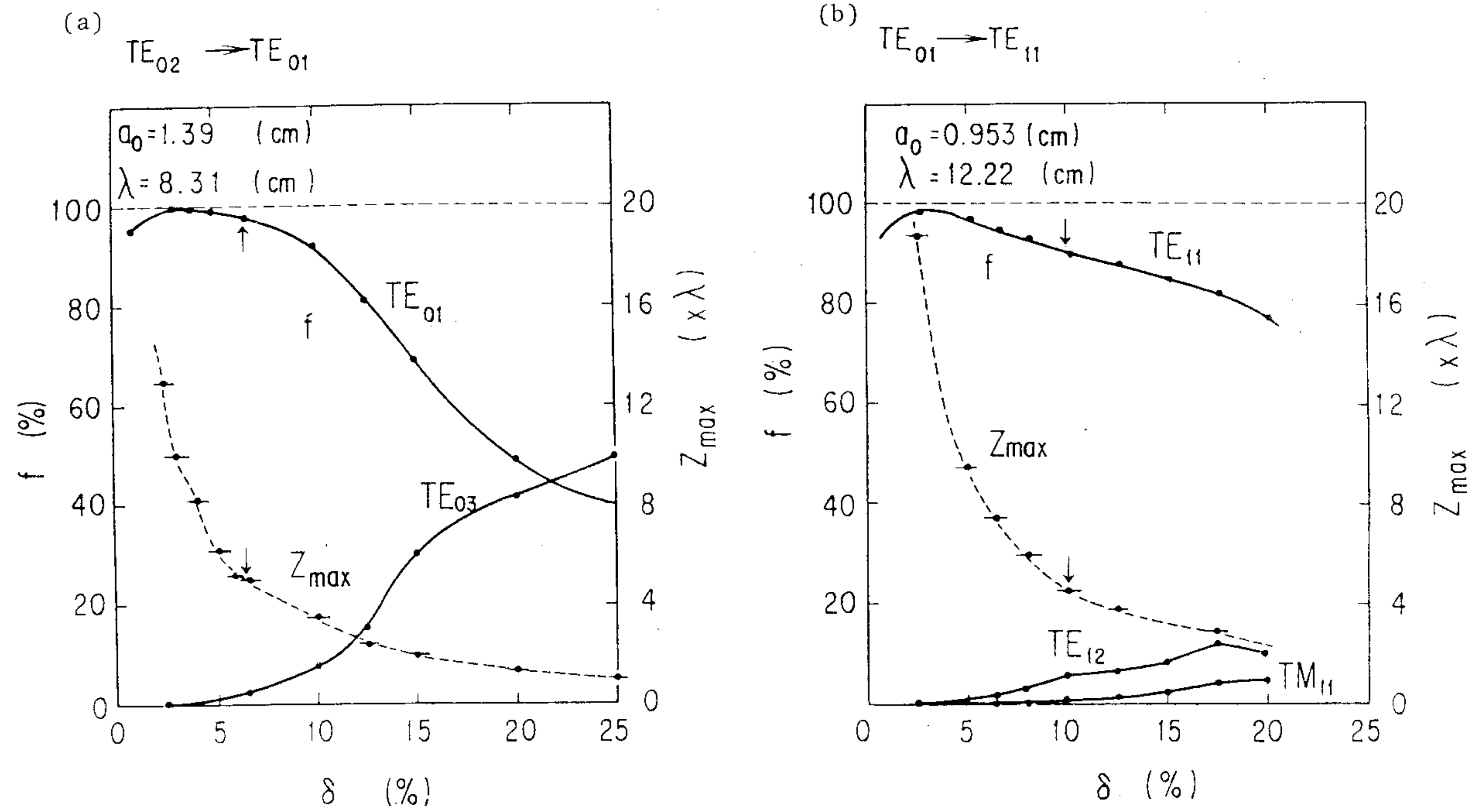

Fig. 5 Conversion efficiency (f) as the function of perturbation amplitude (δ) of

(a) $TE_{02} \rightarrow TE_{01}$ converter

(b) $TE_{01} \rightarrow TE_{11}$ converter

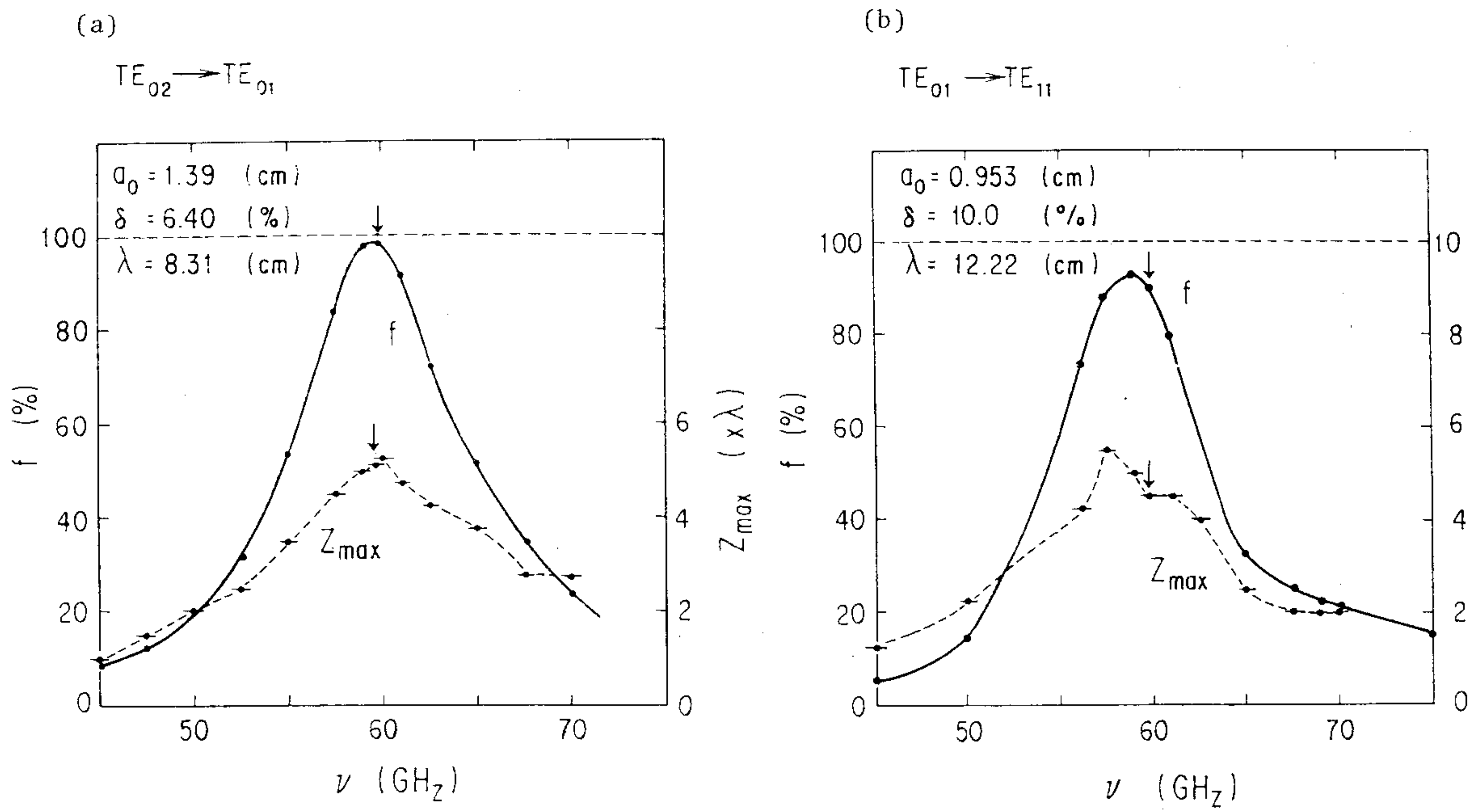

Fig. 6 Frequency characteristics of

(a) $TE_{02} \rightarrow TE_{01}$ converter

(b) $TE_{01} \rightarrow TE_{11}$ converter

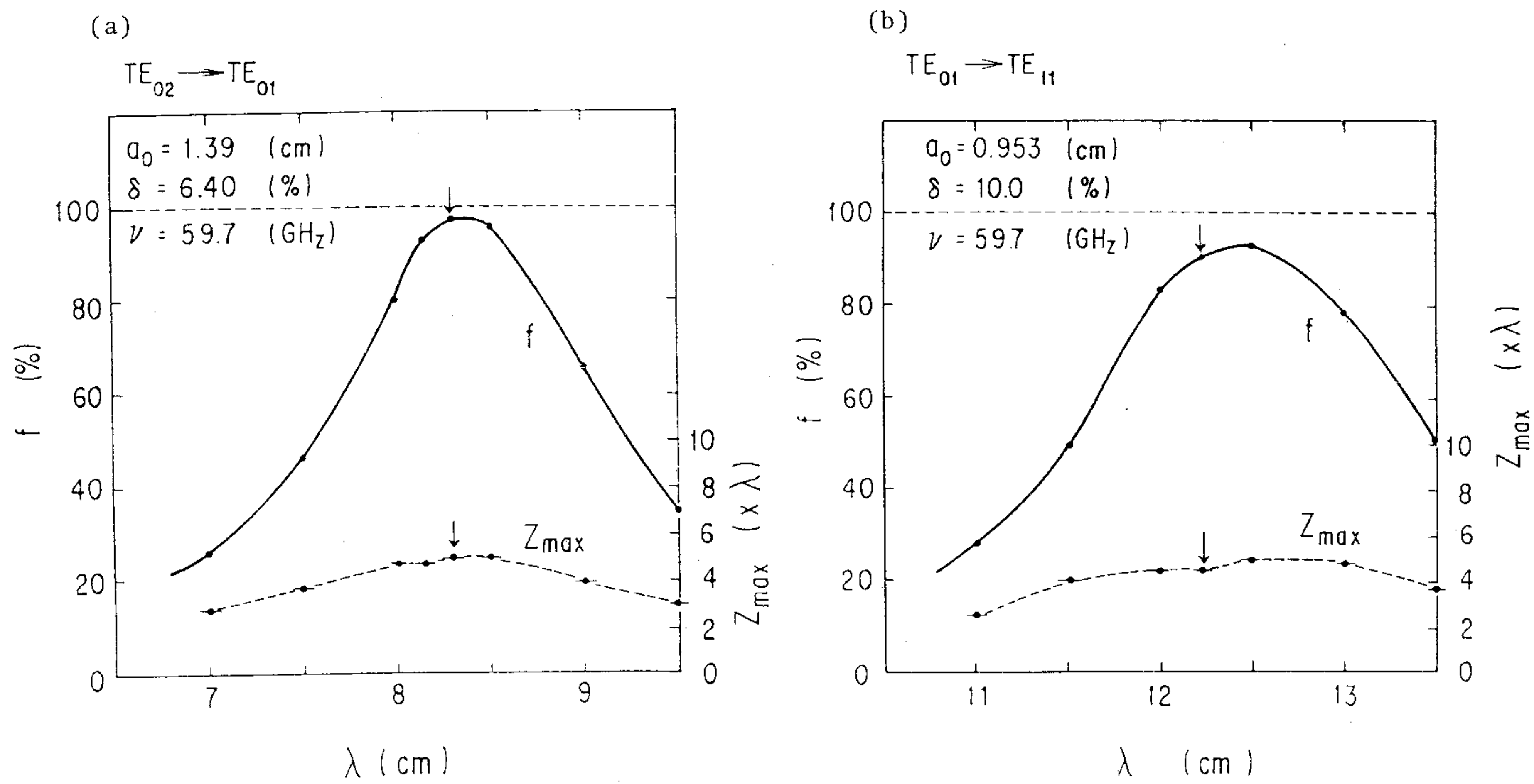

Fig. 7 λ dependence of

(a) $TE_{02} \rightarrow TE_{01}$ converter

(b) $TE_{01} \rightarrow TE_{11}$ converter

Table 1 Input parameters

1	type of mode converter	;	A, B, C	
2	radius of the waveguide	;	$a_0(Z)$	(m)
3	magnitude of the perturbation	;	δ	(%)
4	wave length of the perturbation	;	λ	(m)
5	frequency	;	ν	(Hz)
6	length of the converter	;	Z	(m)
7	initial mesh width	;	ΔZ	(m)
8	parameter for convergence	;	ε	
9	identification of mode to be calculated			
10	input mode			
11	period of print out	;	ΔZp	(m)

Table 2 Output parameters

a) Output of line printer

1	input data		
2	coordinate	;	Z
3	energy in a mode	;	AA(K)
4	total energy	;	TOEN
5	amplitude of a mode	;	YY(K)
6	differential coefficient	;	FF(K)
7	width of mesh	;	H

b) Graphic output

1 type of converter
2 amplitude of wave
3 shape of the converter
4 a_0, δ, λ

Table 3 Obtained size of the converters

type	frequency ν (GHz)	radius a_0(cm)	wave length of perturbation λ (cm)	magnitude of perturbation δ (%)	length Z_{max}(cm)	conversion efficiency f (%)	parasitic modes
$TE_{02} \to TE_{01}$	59.7	1.39	8.31	6.4	41.6 (5.0λ)	98.0	TE_{03}
$TE_{01} \to TE_{11}$	59.7	0.95	12.22	10.0	55.0 (4.5λ)	90.0	TE_{12} TM_{11}

Table 4 Accuracy

type	allowable error in f	error in perturbation $\Delta(a_0\ \delta)$ (mm)	error in wave length $\Delta\lambda$ (mm)
A	± 5 %	± 0.85	± 1.75
$TE_{02} \to TE_{01}$	± 1 %	± 0.21	± 0.95
B	± 5 %	± 0.33	± 1.50
$TE_{01} \to TE_{11}$	± 1 %	± 0.048	± 0.50